Available online at www.sciencedirect.com
ScienceDirect
Journal of the European Ceramic Society 31 (2011) 2073–2081
www.elsevier.com/locate/jeurceramsoc

Process control and optimized preparation of porous alumina ceramics by starch consolidation casting

E. Gregorová, W. Pabst *

Department of Glass and Ceramics, Institute of Chemical Technology, Prague, Technická 5, 166 28 Prague 6, Czech Republic

Received 15 February 2011; received in revised form 4 May 2011; accepted 16 May 2011

Abstract

This work concerns details of porosity and pore size control in starch consolidation casting of alumina ceramics using corn starch. In particular, the influence of the solids loading (68–78 wt.% alumina in suspensions with nominal starch contents of 20–50 vol.%) on the porosity, bulk density and shrinkage of alumina ceramics is studied. The results indicate a linear decrease of the linear shrinkage and the bulk density (and a corresponding increase in porosity) as the alumina concentration increases, with slopes that are independent of the starch content. The pore size is characterized via microscopic image analysis, the pore throat size via mercury porosimetry. Relations between the volumetric shrinkage, porosity and the volume fractions of starch and water in the suspensions are discussed, and a new concept, called "affine limit porosity" is proposed to explain the apparently paradoxical finding that the porosity increases with increasing alumina content in the suspension.

Keywords: A. Slip casting; B. Microstructure-final; B. Porosity; D. Al_2O_3; Pore size

1. Introduction

For more than a decade now the number of publications dealing with the preparation of porous ceramics using starch is steadily growing.[1–19] The constant interest in using starch in ceramic technology indicates that – far from being a purely academic research item – starch is becoming an indispensable commodity for the ceramics industry. While starch has been used as a pore-forming agent for at least 20 years[19] and its use as a binder in industrial extrusion is of an even earlier date,[20,21] the most influential modern key paper in this field has been by Lyckfeldt and Ferreira.[22] In that paper a principally new shaping technique has been presented: starch consolidation casting (sometimes called simply starch consolidation or abbreviated SCC). This method uses the ability of starch to swell and finally gelatinize in water at elevated temperature (60–80 °C), so that ceramic green bodies can be formed from suspensions in impermeable molds (usually metal molds).[22–31] Today SCC has become a competitive shaping technique beside traditional slip casting (into porous molds, typically plaster molds) with starch added as a mere pore former. The main advantage of using starch in ceramic technology, in contrast to many other biopolymers and natural polysaccharides (e.g. poppy seed[32,33] and carrageenan[34,35]), consists in their chemical purity (elements C, H, O with only traces of other elements), which guarantees residual-free (i.e. ash-free) burnout.[28–31] A specific advantage for porous ceramics is the fact that the pore size can be controlled by choosing the appropriate starch type and that the pore size distribution is in most cases sufficiently narrow to make technological process control efficient.

Starches are natural biopolymers from different botanical sources. The most popular commercial starch types are rice, corn (maize), tapioca (cassava), wheat and potato starch, but starches from other cereal types (e.g. rye, barley), vegetables (e.g. peas, lentils, beans) and fruits (e.g. banana) are also available to a limited extent. The size and shape of the starch granules and their properties are primarily determined by the plant genotype, but the influence of the environment (soil, climate) is non-negligible. Of course, modern starch refining technologies ensure relatively high quality standards and more or less constant composition, characteristics (size and shape) and properties. Nevertheless, the size distribution curves of starches from different producers can be quite different, depending on the details of the starch refining technology. For example, cereal starches such as wheat,

* Corresponding author.
E-mail addresses: pabstw@vscht.cz, Willi.Pabst@vscht.cz (W. Pabst).

0955-2219/$ – see front matter © 2011 Elsevier Ltd. All rights reserved.
doi:10.1016/j.jeurceramsoc.2011.05.018

rye and barley, typically contain two types of starch granules, large ones (so-called "A-fraction" or "A-starch") and smaller ones (so-called "B-fraction" or "B-starch"), which may result in clearly bimodal size distributions,[36] and different producers can be more or less successful in eliminating the B-fraction. The A- and B-fractions exhibit differences with respect to chemical composition, the amylopectin ultrastructure, the amylopectin arrangement in the starch granule and many related properties.[37] Size and composition also play key roles in determining the rheological properties of starch-containing suspensions and the viscoelastic behavior (corresponding to swelling and gelatinization) of starch in aqueous media at elevated temperature.[38] Therefore, once the starch type is selected it is necessary to adapt and fine-tune the processing route.

The present work deals with this kind of process optimization for the preparation of porous alumina ceramics with corn starch. Corn starch is probably the most frequently used starch type because of its intermediate size (with median diameters typically around 14 μm), narrow size distribution and isometric shape.[36] The characteristics of tapioca (cassava) starch are very similar.[36] For comparison, rice starch is significantly smaller (so that its pores have a greater tendency to shrink during firing), wheat starch has a bimodal size distribution and potato starch is larger and more anisometric.[36] Although the starch type and content is of primary importance for the resulting microstructure of porous ceramics, other parameters cannot be neglected. In this paper we focus on the influence of the ceramic powder content (i.e. the alumina concentration) in the ceramic suspension, since in practice it is always necessary to adapt the ceramic powder concentration to the starch content in the suspension to attain sufficient fluidity of the suspension. In particular, in this paper we solve an intricate and subtle problem, which arises from the reproducible finding that for increasing alumina content in the suspensions the porosity of the ceramics increases (although the starch content has been kept constant). We will show that this apparently paradoxical finding, which has been tacitly ignored (if noticed at all) by other authors, has a plausible explanation.

2. Theoretical

In order to build process control on a solid fundament it is first of all necessary to precisely define the concentration measures used. Although trivial in principle, the fact that a starch-containing suspension is (in the simplest case) a three-phase system (alumina, water, starch) has to be taken into account for concentration calculations. In particular, this implies the possibility of choosing different concentration measures, often complicating a direct comparison of different authors' results. In this paper (and in all our previous papers) we use the following concentration measures: the alumina content in the suspensions is always given by its weight (or mass) fractions X_A or the corresponding weight (or mass) percentages [wt.%] related to water (i.e. not taking account of the starch added), while the starch content is always given in volume fractions ϕ_S (or the corresponding volume percentages [vol.%]) related to the ceramic powder (here alumina). The reason for this choice, which we believe to be the most rational one, is that the alumina content in wt.% related to water, i.e.

$$X_A = \frac{m_A}{m_A + m_W}, \tag{1}$$

where m_A is the mass of alumina and m_W is the mass of water, serves directly as a recipe for preparing aqueous stock suspensions, to which different amounts of starch may added afterwards, whereas the starch content in vol.% related to the ceramic powder (and not to the suspension as a whole), i.e.

$$\phi_S = \frac{V_S}{V_S + V_A}, \tag{2}$$

where V_S is the volume of starch and V_A is the volume of alumina, can be directly compared with the porosity of the resulting ceramics after firing, because in the absence of swelling and shrinkage this starch content (we call it the "nominal starch content", because it is not the starch content related to the suspension as a whole) directly determines the total porosity after firing (when the matrix between the starch-made pores is densely sintered).

Assuming that the firing shrinkage is determined solely by the intergranular matrix porosity (i.e. the large pores resulting from starch burnout do not actively contribute to shrinkage) and the matrix is densely sintered after firing, the total porosity ϕ can be predicted using the Slamovich–Lange relation[39]:

$$\phi = \frac{\phi_S \rho_{rA}}{1 - \phi_S + \phi_S \rho_{rA}}, \tag{3}$$

where ρ_{rA} is the relative density (packing fraction) of the alumina matrix after drying and starch burnout, but before sintering. Note that in the limit $\rho_{rA} \to 1$ (i.e. a matrix packing fraction approaching 100% before sintering) the total porosity predicted approaches the nominal starch content, i.e.

$$\phi \to \phi_S \quad \text{for} \quad \rho_{rA} \to 1. \tag{4}$$

Thus, under the assumptions made in the Slamovich–Lange model, this is an upper bound. For more realistic ρ_{rA} values, however, the total porosity predicted by the Slamovich–Lange model would be lower than the nominal starch content. In cases where the ρ_{rA} value cannot be determined experimentally, the random close packed (or better "maximally random jammed") value for monodisperse spheres ($\rho_{rA} = 0.64$) appears to be the most reasonable choice. Note, however, that in the Slamovich–Lange model a possible swelling of the pore-forming agent is not taken into account.

The volume fractions of alumina in the alumina–water system ϕ_A can be calculated from the weight fractions X_A via the densities of alumina ($\rho_A = 4.0\ \mathrm{g/cm^3}$) and water ($\rho_W = 1.0\ \mathrm{g/cm^3}$) using the relation:

$$\phi_A = \frac{V_A}{V_A + V_W} = \frac{X_A}{\rho_A}\left[\frac{X_A}{\rho_A} + \frac{(1 - X_A)}{\rho_W}\right]^{-1}, \tag{5}$$

where V_W is the volume of water. Thus, for example, the volume fractions of alumina for aqueous suspensions with 68 and 78 wt.% alumina are 34.7 and 47.0 vol.%, respectively. A starch

density of 1.5 g/cm^3 can be assumed for all starches to calculate the mass of starch to be weighed in. Now both the volume of starch V_S and the volume of water V_W can be expressed in terms of the alumina volume and the volume fractions ϕ_S and ϕ_A, respectively, i.e.

$$V_S = V_A \cdot \frac{\phi_S}{1-\phi_S}, \tag{6}$$

and

$$V_W = V_A \cdot \frac{1-\phi_A}{\phi_A}. \tag{7}$$

From these we obtain the volume fraction of starch in the suspension as a whole ϕ'_S as:

$$\phi'_S = \frac{V_S}{V_S + V_A + V_W} = \frac{\phi_A \phi_S}{1 - \phi_S + \phi_A \phi_S}, \tag{8}$$

and the volume fraction of the sum of water and starch in the suspension ϕ'_{W+S} as:

$$\phi'_{W+S} = \frac{V_W + V_S}{V_S + V_A + V_W} = \frac{1 - \phi_A - \phi_S + 2\phi_A\phi_S}{1 - \phi_S + \phi_A \phi_S}. \tag{9}$$

Accordingly, the volume fraction of alumina in the starch-containing suspension ϕ'_A is:

$$\phi'_A = \frac{V_A}{V_S + V_A + V_W} = 1 - \phi'_{W+S} = \frac{\phi_A - \phi_A\phi_S}{1 - \phi_S + \phi_A \phi_S}. \tag{10}$$

The significance of Eq. (7) consists in the fact that it determines the free volume that is not occupied by ceramic powder. This volume is initially occupied by a mixture of starch granules and water and finally – in accordance with the principle of the SCC process[22] – by swollen and gelatinized starch. If shrinkage could be neglected, this would be exactly the total porosity to be expected in the ceramic body after firing. Of course, shrinkage cannot be neglected when the body is to have satisfactory strength, i.e. when the matrix between the pores is to be more than only partially sintered. In order to take this effect into account it is necessary to determine the volumetric shrinkage σ_V, defined as:

$$\sigma_V = \frac{V_0 - V}{V_0}, \tag{11}$$

where V_0 is the volume of the as-shaped green body before firing and V is the body volume after firing. If isotropic (directionally independent) shrinkage is assumed, the volumetric shrinkage can be calculated from the readily measurable linear shrinkage S via the relation:

$$\sigma_V = 3S - 3S^2 + S^3. \tag{12}$$

We would like to emphasize that the shrinkage is almost completely determined by the matrix between the large pores. In other words, the very small, concave interstitial voids between the ceramic particles cause essentially all the shrinkage of the ceramic body. It is a well-known fact that large pores in a fine-grained matrix do not by themselves contribute to shrinkage.[40,41] They do shrink, of course, as dictated by the overall shrinkage of the body (caused almost exclusively by the matrix), but it has to be emphasized that their size reduction does not reduce the porosity of the ceramic body. When shrinkage and total porosity after firing are known by measurement, we may reconstruct the initial porosity that the body had before firing. Of course this is a hypothetical value, because before high-temperature heat treament the future pores were partly or totally filled with gelatinized starch, and the value thus calculated characterizes the state of the body before strengthening by (at least partial) sintering. Therefore we call this quantity, in analogy to affine mappings in mathematics, an "affine limit porosity". It is calculated via the following relation (see Appendix A for a derivation of this relation):

$$\phi_{ALP} = \sigma_V + (1 - \sigma_V)\phi, \tag{13}$$

where ϕ is the total porosity measured in the as-fired ceramic body. The physical and practical meaning of this quantity is that it remains constant in the course of sintering, i.e. it is an invariant for a certain composition and can be used to characterize a body with a given composition in each stage of (partial or complete) sintering. It is based on the plausible fact that porosity and shrinkage are intimately connected: the higher one, the lower the other. Moreover, if it is assumed that volume conservation is approximately fulfilled during starch swelling and gelatinization, the affine limit porosity of the porous ceramic body of given composition should be equal to the volume fraction of starch and water in the suspension given in Eq. (9) above, i.e.

$$\phi_{ALP} = \phi'_{W+S}. \tag{14}$$

That means, in the SCC process the affine limit porosity can be predicted based only on the composition of the suspension. On the other hand, this theoretical prediction can be verified by independent measurements (of porosity and shrinkage). The experimental verification of this theoretical model will be given below.

3. Experimental

Aqueous suspensions for casting were prepared with commercial submicron alumina powder CT 3000 SG (Almatis, Germany), corn starch (Gustin, Dr. Oetker, Czech Republic), an alkali-free deflocculant (Dolapix CE 64, Zschimmer & Schwarz, Germany) and distilled water. The suspensions were homogenized in polyethylene bottles with 8-mm-diameter alumina balls for 2 h on a laboratory shaker (HS 260, IKA, Germany) at a frequency of 5 Hz. The amount of deflocculant added was 1 wt.% related to Al_2O_3. The alumina concentration in the suspensions was calculated using a density value of 4.0 g/cm^3 for alumina and 1.0 g/cm^3 for water. The amount of starch (nominal starch content, related to alumina) was calculated using a density value of 1.5 g/cm^3 for starch. Before casting the suspensions were ultrasonicated (UP 200 S, Dr. Hielscher, Germany) to support deagglomeration and to eliminate air bubbles. The metal molds used, see Fig. 1, have a cylindrical cavity of diameter 7 mm and length 80 mm. Before casting they were heated up to 45 °C

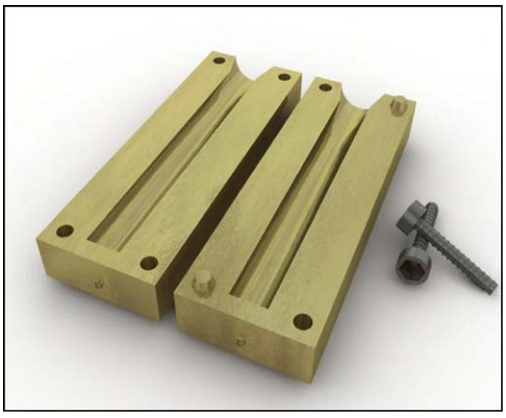

Fig. 1. Metal molds used for starch consolidation casting.

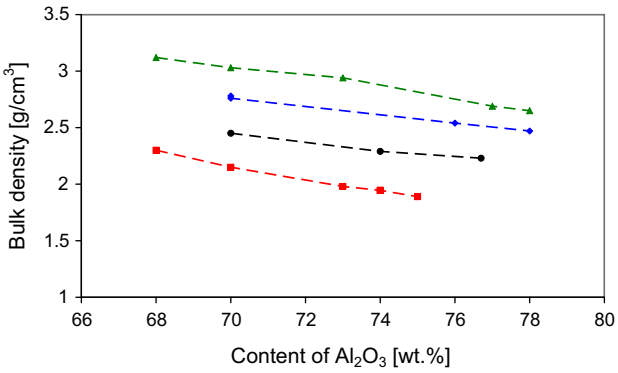

Fig. 2. Bulk density of porous alumina ceramics prepared from suspensions with nominal starch contents of (from top to bottom) 20 vol.% (triangles), 30 vol.% (diamonds), 40 vol.% (circles) and 50 vol.% (squares).

and the inner surface coated with an alkali-free grease to aid demolding of the ceramic green bodies. After casting of suspensions into the molds, they were put into a laboratory drier preheated to 80 °C for 2 h. After subsequent cooling to room temperature the molds were openend and dried in the drier with a stepwise increase in temperature (60, 80 and 105 °C), with a 2 h dwell at the intermediate temperatures. Firing was performed at 1570 °C according to a standard schedule (heating rate 2 °C/min, 2 h dwell at maximum temperature), i.e. without any special dwell for starch burnout. The as-fired samples were characterized with respect to bulk density and porosity (open and total) via the Archimedes method (boiling in water for 2 h and soaking overnight), and the shrinkage was determined via a slide caliper. Polished sections were prepared to obtain micrographs by optical microscopy (Jenapol, Zeiss, Germany) and perform image analysis (Lucia G, Laboratory Imaging, Czech Republic). Image analysis was performed by manually marking pore sections by area-equivalent circles (at least 1100 objects for each sample) and transforming the number-weighted distribution to a volume-weighted one under the assumption of a size-invariant shape, cf.[42]. Selected samples were investigated by mercury porosimetry (AutoPore IV 9500, Micrometrics, USA). In order to enable a direct comparison with the image analysis results the intrusion curves were rescaled to 100%, cf.[43].

4. Results and discussion

Table 1 lists the compositions of the suspensions used. From each suspension at least five specimens have been prepared, and shrinkage, bulk density, open and total porosity values are given as arithmetic means with standard deviations. The influence of the alumina and starch contents on bulk density, open and total porosity are shown in Figs. 2–5. Figs. 2 and 3 show, for a given nominal starch content, the dependence of bulk density and porosity (open and total) on the alumina concentration (mass percentage related to water). The dependences are almost linear and can be fitted by linear regression. Fit relations for the bulk density ρ [g/cm^3] and the total porosity ϕ [%] as a function of the alumina content in the suspension X_A [wt.%] (valid in the range 68 vol.% > X_A > 78 vol.%) are

$$\rho = a + b \cdot X_A, \tag{15}$$

Table 1
Composition of suspensions, shrinkage and microstructural characteristics of the porous alumina ceramics.

Nominal starch content [vol.%]	Alumina content [wt.%]	Bulk density [g/cm^3]	Apparent (open) porosity [%]	Total porosity [%]	Linear shrinkage [%]
20	68	3.12 ± 0.08	16.2 ± 2.3	22.1 ± 2.0	29.1 ± 0.6
20	70	3.03 ± 0.06	18.9 ± 1.6	24.3 ± 1.6	25.9 ± 0.5
20	73	2.94 ± 0.08	23.7 ± 2.1	26.6 ± 1.8	21.9 ± 0.8
20	77	2.69 ± 0.09	30.8 ± 2.9	32.7 ± 2.2	16.5 ± 1.0
20	78	2.65 ± 0.01	31.0 ± 0.3	33.8 ± 0.3	14.7 ± 0.8
30	70	2.78 ± 0.04	29.0 ± 1.0	30.6 ± 0.9	25.0 ± 0.5
30	70	2.76 ± 0.04	28.8 ± 0.9	30.8 ± 1.0	24.1 ± 0.7
30	76	2.54 ± 0.02	35.7 ± 0.5	36.6 ± 0.5	17.9 ± 0.4
30	78	2.47 ± 0.01	35.6 ± 0.1	38.2 ± 0.2	15.1 ± 0.3
40	70	2.45 ± 0.03	38.3 ± 0.6	38.6 ± 0.7	24.3 ± 0.6
40	74	2.29 ± 0.01	42.4 ± 0.2	42.7 ± 0.2	19.4 ± 0.5
40	77	2.23 ± 0.01	43.9 ± 0.3	44.2 ± 0.3	16.4 ± 0.5
50	68	2.30 ± 0.02	41.8 ± 0.3	42.4 ± 0.4	23.8 ± 0.3
50	70	2.15 ± 0.03	45.4 ± 0.8	46.2 ± 0.6	21.7 ± 0.2
50	73	1.98 ± 0.03	50.1 ± 0.3	50.6 ± 0.3	17.0 ± 0.3
50	74	1.96 ± 0.04	51.0 ± 1.1	51.4 ± 1.1	16.1 ± 0.2
50	75	1.89 ± 0.03	52.0 ± 0.6	52.8 ± 0.8	15.4 ± 0.5

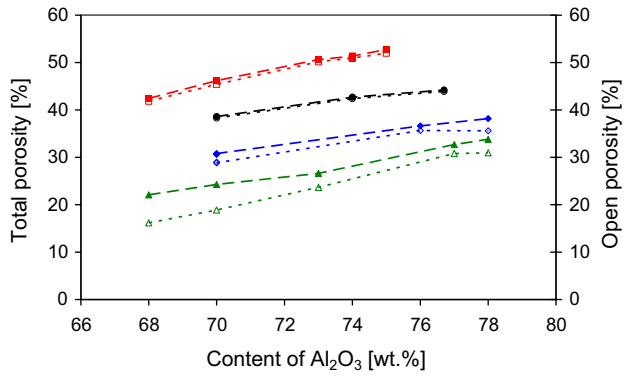

Fig. 3. Total porosity (full symbols, left ordinate) and apparent, i.e. open, porosity (empty symbols, right ordinate) of porous alumina ceramics prepared from suspensions with nominal starch contents of (from bottom to top) 20 vol.% (triangles), 30 vol.% (diamonds), 40 vol.% (circles) and 50 vol.% (squares).

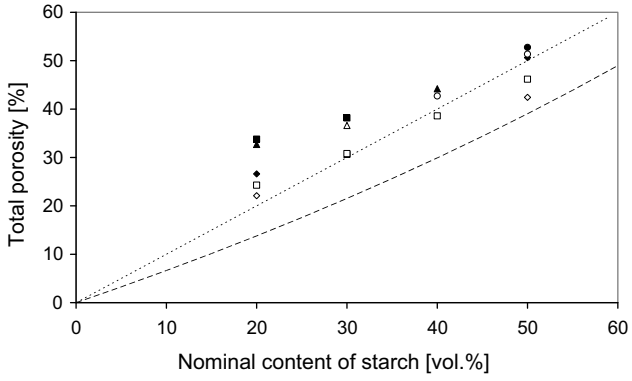

Fig. 4. Total porosity of as-fired alumina ceramics in dependence of the nominal starch content in the suspensions for different alumina contents (empty diamonds – 68 wt.%, empty squares – 70 wt.%, full diamonds – 73 wt.%, empty circles – 74 wt.%, full circles – 75 wt.%, empty triangles – 76 wt.%, full triangles – 77 wt.%, full squares – 78 wt.%); the dotted line and the dashed curve are guides to the eye, corresponding to the theoretically expected porosity in the absence of swelling (dotted line: porosity according to Eq. (4) for the limit matrix packing fraction of 100% before firing – in this case the porosity would be equal to the nominal starch content; dashed curve: porosity according to the Slamovich–Lange relation, Eq. (3), for an assumed matrix packing fraction of 0.64).

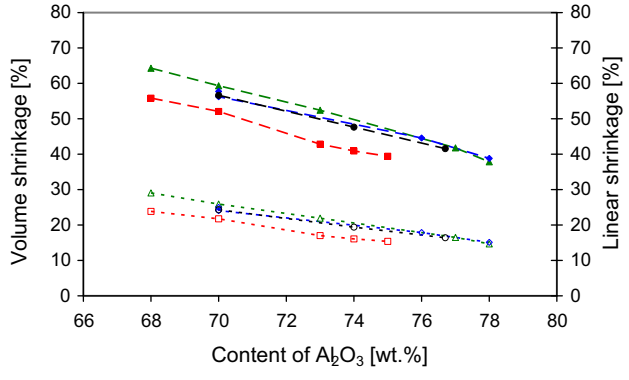

Fig. 5. Volume shrinkage (full symbols, left ordinate), calculated from the measured linear shrinkage (empty symbols, right ordinate) under the assumption of isotropy, of porous alumina ceramics prepared from suspensions with nominal starch contents of (from top to bottom) 20 vol.% (triangles), 30 vol.% (diamonds), 40 vol.% (circles) and 50 vol.% (squares).

and

$$\phi = c + d \cdot X_A, \tag{16}$$

respectively, with the fit parameters a ranging from 4.8 to 6.4, b (slope) ranging from −0.033 to −0.058 (with correlation coefficients 0.979–0.997), c ranging from −20.7 to −56.3 and d (slope) ranging from 0.85 to 1.46 (with correlation coefficients 0.978–0.998). It is evident that the slopes are similar irrespective of the nominal starch content. This dependence on the alumina content is typical for starch consolidation casting (SCC) and in contrast to traditional slip casting (TSC, with or without starch). Fig. 4 shows that the porosity achieved in SCC does not obey the Slamovich–Lange prediction, Eq. (3) (many values are even above the upper bound – dotted line); as expected, the porosity achieved is higher (because of starch swelling) and depends on the alumina content in the suspension – an influence which is not considered in the Slamovich–Lange model.[39] Also the skrinkage exhibits a clear trend with alumina concentration (Fig. 5), and both the linear and the volumetric shrinkage exhibit more or less a linear decrease with the alumina weight percentage related to water, which can be fitted by linear regression. Fit relations for the linear shrinkage S [%] and the volumetric shrinkage σ_V [%] as a function of the alumina content in the suspension X_A [wt.%] (valid in the range 68 vol.% > X_A > 78 vol.%) are

$$S = e + f \cdot X_A, \tag{17}$$

and

$$\sigma_V = g + h \cdot X_A, \tag{18}$$

respectively, with the fit parameters e ranging from 105 to 125, f (slope) ranging from −1.16 to −1.41 (with correlation coefficients 0.989–0.999), g ranging from 212 to 241 and h (slope) ranging from −2.21 to −2.60 (with correlation coefficients 0.983–0.999).

It has to be noted that the finding that in SCC the porosity increases with increasing alumina content in the suspensions is absolutely reproducible. At first sight, however, it might seem paradoxical that the porosity is higher when the solids loading in the suspensions is higher, because it should be expected that starch exhibits a higher degree of swelling when the suspension has a lower alumina content (and thus the starch swelling is less constrained by excluded-volume effects). In order to explain this finding, we invoke our aforementioned concept of the "affine limit porosity" (ALP). As mentioned before, this concept is based on the fact that the shrinkage that has occurred during firing and the residual porosity remaining after firing are complementary quantities: the higher the shrinkage, the lower the porosity. The ALP defined above corresponds to the maximum porosity that could be achieved in a ceramic body if shrinkage could be avoided, e.g. if only non-densifying sintering mechanisms could be activated. Therefore it is a constant characterizing a body of certain composition irrespective of the stage or degree of sintering (partial or complete).

Fig. 6 shows the volume fractions of starch in the suspensions and the sum of the volume fractions of water and starch. The latter is in fact the theoretically expected value of the APL,

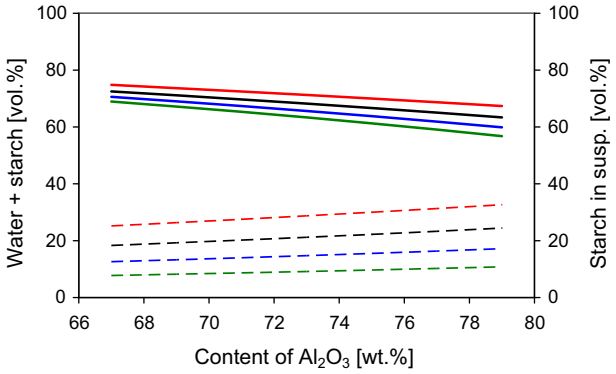

Fig. 6. Volume fractions of water + starch (full symbols, left ordinate) and of starch alone (empty symbols, right ordinate) in the suspensions in dependence of the alumina content.

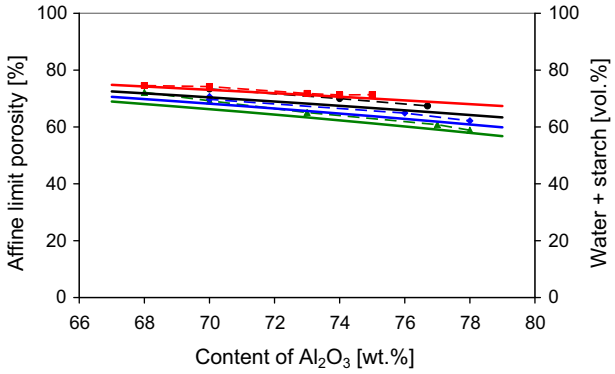

Fig. 7. Comparison of the sum of the volume fractions of water and starch in the suspensions (theoretical prediction based only on the suspension composition) with the affine limit porosities (determined from the measured values of total porosity and shrinkage) of porous alumina ceramics prepared from suspensions with nominal starch contents of (from top to bottom) 20 vol.% (triangles), 30 vol.% (diamonds), 40 vol.% (circles) and 50 vol.% (squares).

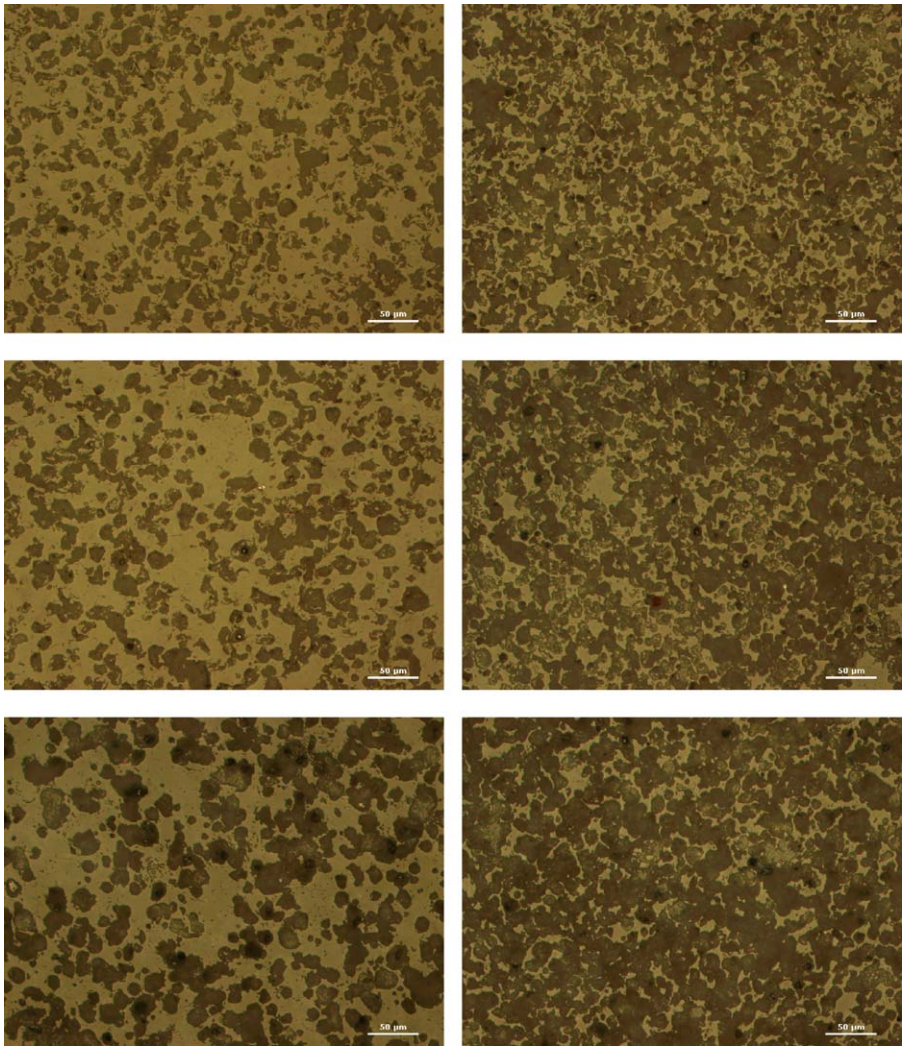

Fig. 8. Micrographs of porous alumina ceramics (polished sections) prepared by SCC from suspensions with nominal starch contents of 20 vol.% (l.h.s.) and 50 vol.% (r.h.s.) and alumina concentrations of 68, 73 and 78 wt.% (l.h.s., from top to bottom) and 68, 73 and 75 wt.% (r.h.s., from top to bottom).

Table 2
Characteristic values (medians and extreme deciles) of the pore size distributions determined via microcopic image analysis and of the pore throat size distributions determined via mercury porosimetry.

	Image analysis			Mercury porosimetry		
	D_{10} [μm]	D_{50} [μm]	D_{90} [μm]	D_{10} [μm]	D_{50} [μm]	D_{90} [μm]
A68C20	7.7	11.4	15.5	0.8	0.7	0.5
A73C20	9.8	12.5	16.6	1.2	0.9	0.5
A78C20	11.0	14.8	18.6	1.2	2.4	2.8
A68C50	6.6	9.9	13.9	1.1	2.0	2.5
A73C50	7.8	11.5	14.4	1.5	2.5	2.9
A75C50	9.4	13.4	17.2	1.6	2.7	3.1

because it is simply "everything" that occupies space (volume) in the three-phase system (green body), except for the ceramic powder (alumina). Fig. 7 compares this theoretical "prediction" (based only on the suspension composition) with the ALP values calculated from the measured porosity and shrinkage values via Eq. (13). The agreement is indeed remarkable, and the decreasing trend of both the theoretical prediction and the experimental values show that the affine limit porosity (ALP) is the quantity that is decreasing with increasing alumina content in the suspension, as expected, and not the measured total porosity that remains in the ceramic body after firing. We note in passing that in assuming a (water-saturated) three-phase system we have excluded air bubbles, and the good agreement in Fig. 7 also demonstrates that this assumption was justified.

It has to be noted that not only the suspension composition, including the alumina concentration in the suspension, but also the shape of the mold may have an influence on the densification via the SCC process, because the principle of this process is an in situ consolidation, where the starch granules swell and press the ceramic particles together (apart from a gluing effect of the gelatinized starch). Important parameters are the surface-to-volume ratio of the mold and the ratio of constrained and free surfaces. In particular, in a mold with a large free surface the bulk density is expected to be absolutely lower, because volume swelling of the starch granules is unconstrained. This has to be taken into account when the SCC process is to be adapted to industrial production.

Fig. 8 shows micrographs of polished sections of porous alumina ceramics prepared by SCC from suspensions with nominal starch contents of 20 and 50 vol.%, respectively. Fig. 9 shows the corresponding volume-weighted pore size distributions (cumulative curves) determined by image analysis, and Table 2 lists the corresponding characteristic pore size values. It is evident that in the SCC process the pore size increases with increasing alumina content and that, for both nominal starch contents, the median values change by approx. 3.5 μm, i.e. by approx. 25% of its maximum value, when the alumina concentration in the stock suspension changes from by approx. 10 wt.%, i.e. from 68 to 78 wt.% (or 75 wt.%; note that for a nominal starch content of 50 vol.% a 78 wt.% alumina suspension would be too viscous for casting). On the other hand, the pore size decreases very slightly with the nominal starch content (the median values decrease by 1-1.5 μm, i.e. by approx. 10% only, when the nominal starch content is changed by approx. 30 vol.%, i.e. from 20 to 50 vol.%.

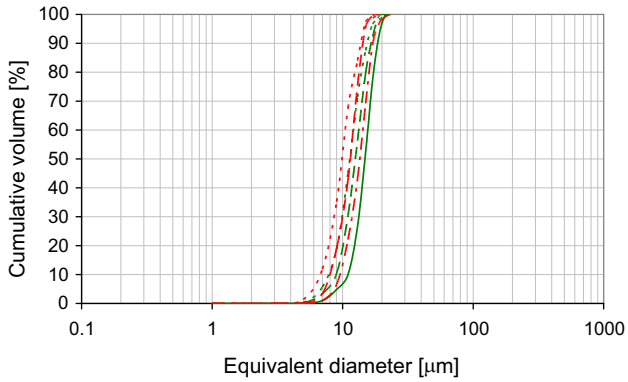

Fig. 9. Pore size distribution determined via microscopic image analysis on polished sections of porous alumina ceramic bodies prepared from suspensions with alumina concentrations of 68, 73, 75 and 78 wt.% (dotted, dashed, dot-dashed and full curve, respectively) and nominal starch contents of 20 vol.% (l.h.s.) or 50 vol.% (r.h.s.).

Fig. 10 confirms the well-known finding[28,29,31,43] that the pore sizes measured by mercury porosimetry are about one order of magnitude lower than those measured by image analysis and have to be interpreted as pore throat size distributions or cell window diameters (in contrast to the cell diameters measured

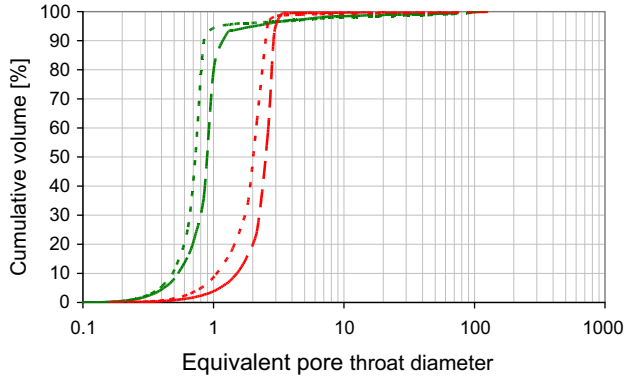

Fig. 10. Pore throat size distribution determined via mercury porosimetry of porous alumina ceramic bodies prepared from suspensions with alumina concentrations of 68 wt.% (dotted) and 73 wt.% (dashed) and nominal starch contents of 20 vol.% (l.h.s.) or 50 vol.% (r.h.s.).

by image analysis). However, while the dependence on the alumina content is similar to that of the pore sizes merasured by image analysis, these results (cf. the characteristic values in Table 2) show a completely different dependence on the nominal starch content compared to the image analysis results: with increasing starch content the sizes of the interconnecting pore throats increase. Nevertheless this is a completely plausible and expected result, because with increasing nominal starch content the pores are coming into closer contact, so that – due to steric hindrance (excluded volume effects) – the pore cavities (cells) become smaller while the pore throats (cell windows) become wider. This investigation shows that essential 3D information can be obtained without tomographical methods when the results are correctly compared and interpreted. In particular, microscopic image analysis and mercury porosimetry have to be considered as complementary tools that are both indispensable for microstructural characterization in general and for the fine-tuning of the SCC process in particular.

5. Summary and conclusion

In this paper it has been shown that using corn starch ($D_{50} = 14$ μm) in the concentration range 20–50 vol.% (nominal starch content, i.e. related to Al_2O_3) porous alumina ceramics with total porosities in the range 22–53% can be prepared via starch consolidation casting (SCC). The total porosity (and open porosity) increases with increasing Al_2O_3 concentration in the suspension (the nominal starch content being unchanged): a change in the Al_2O_3 concentration by 1 wt.% in the suspension gives a change in the total porosity of the fired ceramics by approx. 1 vol.% (i.e. for commonly used alumina suspensions with alumina concentrations in the range 68–78 wt.% the porosity can be varied by approx. 10% only by varying the alumina content). Also the linear shrinkage (and its volumetric counterpart) of as-fired porous alumina ceramics prepared via SCC exhibits a significant dependence on the alumina concentration in the suspensions (in contrast to traditional slip casting), decreasing with increasing Al_2O_3 concentration. The (median) pore size (cell diameter) increases with increasing Al_2O_3 concentration in the suspension (for equal nominal starch contents), as confirmed by microscopic image analysis: a pore size difference of 3.5 μm can be achieved by changing the Al_2O_3 content in the suspension by 10 wt.%; on the other hand, the pore size decreases with increasing starch content when the Al_2O_3 concentration is kept constant. The pore throat size (cell window diameter) increases with increasing Al_2O_3 concentration in the suspension as confirmed by mercury porosimetry; a pore throat size difference of approx. 1–1.5 μm can be achieved by changing the Al_2O_3 content in the suspension by 10 wt.%; note, however, that the pore throat size increases with increasing starch content (in contrast to the aforementioned pore cavities). The apparently paradoxical finding that the porosity of the ceramic after firing increases with increasing alumina content in the suspension, has a plausible explanation when the concept of an "affine limit porosity" (ALP) is introduced: it is found that $\varphi_{ALP} = \varphi'_{W+S}$, i.e. the sum of volume fractions of water and starch in the suspensions (a value calculated directly from the suspension composition) equals the affine limit porosity (a quantity determined from two independently measured values, viz. the total porosity and the volumetric shrinkage). The ALP is an invariant measure of a body's microstructure at arbitrary stages of sintering (partial or complete). It has been shown that microscopic image analysis and mercury porosimetry are tools that provide complementary microstructural information and that both types of results, when correctly compared and interpreted, are indispensable for fine-tuning the SCC process.

Acknowledgements

This study was part of the frame research programme MSM 6046137302 "Preparation and research of functional materials and material technologies using micro- and nanoscopic methods", supported by the Ministry of Education, Youth and Sports of the Czech Republic. Support is gratefully acknowledged.

Appendix A.

From the definition of the volumetric shrinkage σ_V, Eq. (9), it follows that:

$$\frac{V}{V_0} = 1 - \sigma_V, \tag{A1}$$

where V and V_0 are the volumes of the fired ceramic body and the same body in the green state, respectively. On the other hand, the total porosity ϕ (as measured in as-fired ceramic bodies, e.g. using the Archimedes method) is defined as the volume fraction of pores, i.e.

$$\phi = \frac{V_P}{V}, \tag{A2}$$

where V_P is the pore volume after firing. If shrinkage had not occured the pore volume in the body would have been larger by the quantity $(V_0 - V)$, i.e.

$$V'_P = \phi \cdot V + V_0 - V = V(\phi - 1) + V_0. \tag{A3}$$

Therefore, without shrinkage, the porosity would have been:

$$\phi_{ALP} = \frac{V(\phi - 1) + V_0}{V_0} = \frac{V}{V_0}(\phi - 1) + 1 = (1 - \sigma_V)(\phi - 1) + 1 = \sigma_V + (1 - \sigma_V)\phi \tag{A4}$$

("affine limit porosity").

References

1. Corbin SF, Apte PS. Engineered porosity via tape casting, lamination and the percolation threshold of pyrolyzable particulates. *J Am Ceram Soc* 1999;**82**:1693–701.
2. Davis J, Kristoffersson A, Carlström E, Clegg W. Fabrication and crack deflection in ceramic laminates with porous interlayers. *J Am Ceram Soc* 2000;**83**:2369–74.
3. Galassi C, Roncari E, Capiani C, Fabbri G, Piancastelli A, Peselli M, Silvano F. Processing of porous PZT materials for underwater acoustics. *Ferroelectrics* 2002;**268**:47–52.
4. Kim JG, Sim JH, Cho WS. Preparation of porous (Ba, Sr)TiO_3 by adding corn-starch. *J Phys Chem Solids* 2002;**63**:2079–84.

5. Díaz A, Hampshire S. Characterization of porous silicon nitride materials produced with starch. *J Eur Ceram Soc* 2004;**24**:413–9.
6. Mattern A, Huchler B, Staudenecker D, Oberacker R, Nagel A, Hoffmann MJ. Preparation of interpenetrating ceramic–metal composites. *J Eur Ceram Soc* 2004;**24**:3399–408.
7. Reynaud C, Thévenot F, Chartier T, Besson J-L. Mechanical properties and mechanical behaviour of SiC dense-porous laminates. *J Eur Ceram Soc* 2005;**25**:589–97.
8. Barea R, Osendi MI, Ferreira JMF, Miranzo P. Thermal conductivity of highly porous mullite material. *Acta Mater* 2005;**53**:3313–8.
9. Galassi C. Processing of porous ceramics—piezoelectric materials. *J Eur Ceram Soc* 2006;**26**:2951–8.
10. García-Gabaldón M, Pérez-Herranz V, Sánchez E, Mestre S. Effect of porosity on the effective electrical conductivity of different ceramic membranes used as separators in electrochemical reactors. *J Membr Sci* 2006;**280**:536–44.
11. Gregorová E, Živcová Z, Pabst W. Porosity and pore space characteristics of starch-processed porous ceramics. *J Mater Sci* 2006;**41**:6119–22.
12. Živcová Z, Gregorová E, Pabst W, Smith DS, Michot A, Poulier C. Thermal conductivity of porous alumina ceramics prepared using starch as a pore-forming agent. *J Eur Ceram Soc* 2009;**29**:347–53.
13. Živcová Z, Černý M, Pabst W, Gregorová E. Elastic properties of porous oxide ceramics prepared using starch as a pore-forming agent. *J Eur Ceram Soc* 2009;**29**:2765–71.
14. Alves HM, Tarí G, Fonseca AT, Ferreira JMF. Processing of porous cordierite bodies by starch consolidation. *Mater Res Bull* 1998;**33**:1439–48.
15. Lemos AF, Ferreira JMF. Porous bioactive calcium carbonate implants processed by starch consolidation. *Mater Sci Eng C* 2000;**11**:35–40.
16. Rodríguez-Lorenzo LM, Vallet-Regí M, Ferreira JMF. Fabrication of porous hydroxyapatite bodies by a new direct consolidation method: starch consolidation. *J Biomed Mater Res* 2002;**60**:232–40.
17. Pabst W, Týnová E, Mikač J, Gregorová E, Havrda J. A model for the body formation in starch consolidation casting. *J Mater Sci Lett* 2002;**21**:1101–3.
18. Týnová E, Pabst W, Gregorová E, Havrda J. Starch consolidation casting of alumina ceramics—body formation and microstructural characterization. *Key Eng Mater* 2002;**206–213**:1969–72.
19. Bonekamp BC, Schoute MJ, Goris MJAA. Pore properties of ceramic porous media prepared by slip casting of starch-filled α-alumina suspensions. In: de With G, Terpstra RA, Metselaar R, editors. *EuroCeramics: processing of ceramics*, vol. 1. London: Elsevier Applied Science; 1989. p. 223–7.
20. Sikora M, Izak P. Starch and its derivatives in ceramic processing. *Ceramika/Ceramics* 2006;**93**:1–80.
21. Jiang GP, Yang JF, Gao JQ. Effect of starch on extrusion behaviour of ceramic pastes. *Mater Res Innov* 2009;**13**:119–23.
22. Lyckfeldt O, Ferreira JMF. Processing of porous ceramics by "starch consolidation". *J Eur Ceram Soc* 1998;**18**:131–40.
23. Bowden ME, Rippey MS. Porous ceramics formed using starch consolidation. *Key Eng Mater* 2002;**206–213**:1957–60.
24. Týnová E, Pabst W, Mikač J. Starch swelling and its role in modern ceramic shaping technology. *Macromol Symp* 2003;**203**:295–300.
25. Romano P, Velasco FJ, Torralba JM, Candela N. Processing of M2 powder metallurgy high-speed steel by means of starch consolidation. *Mater Sci Eng A* 2006;**419**:1–7.
26. Gregorová E, Pabst W. Porosity and pore size control in starch consolidation casting—achievements and problems. *J Eur Ceram Soc* 2007;**27**: 669–72.
27. Mao X, Wang S, Shimai S. Porous ceramics with tri-modal pores prepared by foaming and starch consolidation. *Ceram Int* 2008;**34**:107–12.
28. Živcová Z, Gregorová E, Pabst W. Low- and high-temperature processes and mechanisms in the preparation of porous ceramics via starch consolidation casting. *Starch/Stärke* 2010;**62**:3–10.
29. Gregorová E, Živcová Z, Pabst W. Starch as a pore-forming and body-forming agent in ceramic technology. *Starch/Stärke* 2009;**61**:495–502.
30. Gregorová E, Živcová Z, Pabst W. Porous ceramics made using potato starch as a pore-forming agent. *Fruit Veg Cereal Sci Biotechnol* 2009;**3**:115–27.
31. Gregorová E, Pabst W, Živcová Z, Sedlářová I, Holíková S. Porous alumina ceramics prepared with wheat flour. *J Eur Ceram Soc* 2010;**30**:2871–80.
32. Gregorová E, Pabst W. Porous ceramics prepared using poppy seed as a pore-forming agent. *Ceram Int* 2007;**33**:1385–8.
33. Živcová Z, Gregorová E, Pabst W. Alumina ceramics prepared with new pore-forming agents. *Process Appl Ceram* 2008;**2**:1–8.
34. Millán AJ, Nieto MI, Moreno R. Near-net shaping of aqueous alumina slurries using carrageenans. *J Eur Ceram Soc* 2002;**22**:297–303.
35. Gregorová E, Pabst W, Štětina J. Viscoelastic behavior of ceramic suspensions with carrageenan. *J Eur Ceram Soc* 2006;**26**:1185–94.
36. Gregorová E, Pabst W, Bohačenko I. Characterization of different starch types for their application in ceramic processing. *J Eur Ceram Soc* 2006;**26**:1301–9.
37. Šárka E, Bubník Z. Morfologie, chemická struktura, vlastnosti a možnost využití pšeničného B-škrobu [Morphology, chemical structure and properties of wheat B-starch and possibilities of its application, in Czech]. *Chem Listy* 2010;**104**:318–25.
38. Gregorová E, Živcová Z, Pabst W, Štětina J, Keuper M. Rheology of ceramic suspensions with organic or biopolymeric gelling additives—Part 3: Suspensions with starch. *Ceram-Silik* 2008;**52**:250–9.
39. Slamovich EB, Lange FF. Densification of large pores: I. Experimental. *J Am Ceram Soc* 1992;**75**:2498–508.
40. Rahaman MN. *Ceramic processing and sintering*. second edition New York: Marcel Dekker; 2003. p. 470–506.
41. German RM. *Sintering theory and practice*. New York: John Wiley and Sons; 1996. p. 67–177.
42. Pabst W, Berthold C, Gregorová E. Size and shape characterization of polydisperse short-fiber systems. *J Eur Ceram Soc* 2006;**26**:1121–30.
43. Gregorová E, Živcová Z, Pabst W, Sedlářová I. Characterization of porous ceramics by image analysis and mercury porosimetry. *Ceramika/Ceramics* 2006;**97**:219–30.